HHS Public Access

Author manuscript

Curr Biol. Author manuscript; available in PMC 2016 June 01.

Published in final edited form as:

Curr Biol. 2015 June 1; 25(11): 1526–1534. doi:10.1016/j.cub.2015.04.025.

A convergent and essential interneuron pathway for Mauthner cell mediated escapes

Alix M.B. Lacoste[1], **David Schoppik**[1,3], **Drew N. Robson**[1,4], **Martin Haesemeyer**[1], **Ruben Portugues**[1,5], **Jennifer M.B. Li**[1,4], **Owen Randlett**[1], **Caroline L. Wee**[2], **Florian Engert**[1], and **Alexander F. Schier**[1,*]

[1]Department of Molecular and Cellular Biology, Harvard University, Cambridge, MA 02138, USA

[2]Program in Neuroscience, Department of Neurobiology, Harvard Medical School, Boston, MA

SUMMARY

The Mauthner cell (M-cell) is a command-like neuron in teleost fish whose firing in response to aversive stimuli is sufficient to produce short-latency escapes [1, 2]. M-cells have been proposed as evolutionary ancestors of startle response neurons of the mammalian reticular formation [3], and studies of this circuit have uncovered important principles in neurobiology that generalize to more complex vertebrate models [4, 5]. The main excitatory input was thought to originate from multisensory afferents synapsing directly onto the M-cell dendrites [5]. Here, we describe an additional, convergent pathway that is essential for the M-cell mediated startle behavior in larval zebrafish. It is composed of excitatory interneurons called spiral fiber neurons, which project to the M-cell axon hillock. By *in vivo* calcium imaging, we found that spiral fiber neurons are active in response to aversive stimuli capable of eliciting escapes. Like M-cell ablations, bilateral ablations of spiral fiber neurons largely eliminate short-latency escapes. Unilateral spiral fiber neuron ablations shift the directionality of escapes and indicate that spiral fiber neurons excite the M-cell in a lateralized manner. Their optogenetic activation increases the probability of short-latency escapes, supporting the notion that spiral fiber neurons help activate M-cell mediated startle behavior. These results reveal that spiral fiber neurons are essential for the function of the M-cell in response to sensory cues and suggest that convergent excitatory inputs that differ

*CONTACT: Correspondence: schier@fas.harvard.edu.

[3]Present address: Neuroscience Institute, New York University Langone School of Medicine, New York, NY 10016, USA

[4]Present address: Rowland Institute, 100 Edwin H Land Blvd, Cambridge, MA 02142, USA

[5]Present address: Max Planck Institute of Neurobiology, Am Klopferspitz 18, Martinsried, Germany

AUTHOR CONTRIBUTIONS: AML, DS and AFS conceived the study. DS generated the *Tg(-6.7FRhcrtR:gal4VP16)* line. AML collected the data. AML analyzed the data with the guidance of DS and discussions with all authors. AML built the behavioral and ChR2 apparatus with help from DNR, DS, MH, CW and RP, and wrote the software with DNR and MH. DNR and JMBL built the two-photon calcium imaging apparatus. OR generated Movie S1. AML and AFS wrote the manuscript with contributions from DS, MH, RP, OR, and FE.

The authors declare no competing financial interest.

in their input location and timing ensure reliable activation of the M-cell, a feedforward excitatory motif that may extend to other neural circuits.

RESULTS

Activity in the M-cells, a pair of large neurons located bilaterally in the hindbrain and projecting directly to motoneurons, is associated with escapes of short latencies [6–9]. Spiral fiber neurons are a group of neurons that project to the contralateral M-cell [10] where they wrap around the axon hillock at a structure called the axon cap [11]. Previous studies suggest that spiral fiber neurons excite the M-cell in adult goldfish [12], and stimulation of a single spiral fiber neuron in larval zebrafish is capable of eliciting an excitatory post-synaptic potential (EPSP) in the contralateral M-cell [10]. Anatomical [11], as well as electrophysiological and pharmacological [10] evidence points to the presence of both glutamatergic and electrical synapses between spiral fiber neurons and the M-cell. Based on these studies, spiral fiber neurons are well positioned to influence the M-cell mediated escape behavior. In fact, mutants for the retinoblastoma-1 gene that have defects in axon targeting, including in the spiral fiber neurons, display abnormal turning movements in response to touch [13, 14]. However, the stimuli that drive the spiral fiber neurons have yet to be identified, and their role in the M-cell escape network remains unclear. Here, we address these questions using functional calcium imaging, ablations, optogenetics and behavior analysis.

Spiral fiber neurons respond to aversive stimuli

We used a transgenic line, *Tg(-6.7FRhcrtR:gal4VP16)*, that labels spiral fiber neurons and other neurons in the larval zebrafish brain (Figure 1A, Movie S1 and Supplemental Methods). In 5-day old larval zebrafish, spiral fiber neurons are a group of ~10 neurons located bilaterally in rhombomere 3, rostro-ventral of the M-cells. These neurons all have descending projections to the contralateral M-cell axon cap and do not appear to contact other targets [10]. We first asked whether spiral fiber neurons are capable of sensing stimuli that are classically used to elicit M-cell dependent escapes (Figure 1B). In paralyzed animals embedded in agarose, we monitored calcium dynamics in spiral fiber neurons labeled with the genetically encoded calcium indicator GCaMP-HS [15] by two-photon microscopy. We first assessed activity in the spiral fiber neuron axon terminals that wrap around the M-cell axon hillock (Figure 1B). We observed irregular and infrequent spontaneous activity in spiral fiber neurons, at a rate of about one calcium event per minute (Figure 1B). We then stimulated the animals with three different stimuli: two tactile stimuli consisting of short water pulses delivered either to the otic vesicle (which develops into the ear) [8] or to the tail [7, 16]. The third stimulus we used was a primarily auditory/vibrational stimulus consisting of an abrupt tap on the dish holding the animal (similar to [9]). We observed that all three types of stimuli elicited robust responses in the spiral fiber neuron axon terminals (Figure 1B). These responses were independent of M-cell activity: after bilateral M-cell ablations, spiral fiber neurons continued to respond to the tap stimulus with comparable amplitude (Figure S1). Thus, spiral fiber neurons encode a range of sensory information.

M-cells respond to stimuli arriving ipsilaterally on their dendrites but individual spiral fiber neurons cross the midline and project to the contralateral M-cell. We thus asked whether the responses of spiral fiber neurons were lateralized accordingly. Consistent with their contralateral projections, we observed that spiral fiber neuron somata were strongly activated by ear and tail stimuli delivered on the contralateral side (Figures 1C and 1D). Ipsilateral spiral fiber neurons also responded but more weakly (ear stimuli: $n = 10$ fish, $p < 0.05$ contralateral vs. ipsilateral; tail stimuli: $n = 10$, $p < 0.05$, Wilcoxon rank sum test), an effect likely due to directional stimuli also being capable of stimulating the opposite side of the skin to a lesser extent. Responses to the non-directional tap stimulus, on the other hand, were not lateralized (Figure 1D, $n = 4$, $p > 0.05$). These results indicate that spiral fiber neurons receive contralateral sensory input, and as they cross the midline, the laterality of sensory information is preserved across M-cell inputs (Figure 1E).

Spiral fiber neuron ablations largely abolish M-cell dependent short-latency escapes

To investigate whether spiral fiber neurons affect the escape behavior, we built an apparatus designed to elicit and quantify escapes in response to an aversive stimulus. 5–7 day old fish were embedded in agarose and their tails were freed. A mechanical tapper hit the plate onto which the fish was placed, in a similar manner to the tap stimulus used for calcium imaging experiments. By imaging at 1000Hz, we were able to reconstruct the curvature of the tail as a function of time, and measure the direction, angle and latency of the response (Figure 2A). The tap stimulus elicited responses with 100% probability ($n = 50$ larvae). The vast majority (99.7%) of these responses were escapes, with latencies ranging from 5 - 25 ms (9.9 ± 0.19 ms, mean ± standard error of the mean). Characteristic escapes consisted of a sharp angle C-bend of the tail (>60°), followed by a counter turn in the oppo site direction and subsequent swimming lasting hundreds of milliseconds (Figure 2A). In accordance with previous findings [9, 17], we classified escapes as either short-latency (≦12 ms) or long-latency (13 - 25 ms). Larvae produced short-latency escapes with a high probability (92 ± 1.4%) whereas long-latency escapes were observed infrequently (8.2 ± 1.4%). Responses with latencies above 25 ms (0.26 ± 0.19%) corresponded to other types of movements such as swims and turns. To uncover the types of sensory systems activated by the tap stimulus, we measured tap responses in fish with nonfunctional hair cells (*mariner* mutants, [18]) and in fish in which the lateral line was ablated by neomycin treatment [19]. Our results indicate that short-latency escapes, but not long-latency escapes, are primarily mediated by the ear, while the lateral line does not play a role (Figure S2). Thus, tap stimuli engage several sensory systems, including the ear. To analyze the respective contributions of the M-cell and spiral fiber neurons to the escape behavior, we compared the response to taps of larvae before and after three ablation conditions: M-cells (Figure 2B), spiral fiber neurons (Figure 2E) or ablation of other neurons in the area as a control (Figure 2H). Targeted ablations were carried out using a pulsed infrared laser as described previously [20]. Previous studies have shown that short-latency escapes in response to auditory stimuli require the M-cells but tactile stimuli only partially depend on the M-cells [7, 8, 16, 21]. Two sets of segmental homologs are thought to elicit escapes of longer latency when the M-cell does not fire [7, 8, 22]. Thus, due to the multisensory nature of our stimulus, we expected the M-cells to be partially required for short-latency escapes. Indeed, we found that after M-cell ablations, the number of short-latency escapes performed decreased in favor of long-latency escapes (n =

14 fish, Figure 2C). The mean probability of short-latency escapes decreased on average 1.8-fold and long-latency escapes increased 3-fold ($p < 0.05$, Wilcoxon signed rank test, Figure 2D). Spiral fiber neuron ablations had a similar effect: after ablations, the majority of escapes observed were long-latency (Figure 2F). Short-latency escapes were reduced by 6-fold and long-latency escapes increased 8.1-fold ($n = 13$, $p < 0.05$, Figure 2G). Control ablations did not induce a change in the escape latency profile (Figure 2I) or probability of escapes ($n = 23$, $p > 0.05$, Figure 2J). The overall probability of response was not affected by any of the ablation procedures (Figures 2D, 2G and 2J).

To compare the effect of ablation across groups, we evaluated the change in short-latency escape probability after ablations. The effects of M-cell and spiral fiber neuron ablations were significantly different from controls ($p < 0.05$, Wilcoxon rank sum test, Figure 2K). A fraction of M-cell ablations did not produce a strong effect, likely due to compensatory escape pathways. Nevertheless, the effects of M-cell and spiral fiber neuron ablations were not statistically distinguishable from each other ($p > 0.05$). Taken together, these experiments show that the phenotype following ablation of the spiral fiber neurons is similar to that of ablating the M-cells, indicating that spiral fiber neurons play an essential role in M-cell mediated escapes.

Spiral fiber neurons are involved in the laterality of M-cell mediated escapes

M-cells provide excitation to the contralateral side of the spinal network, resulting in contralateral tail bends. Due to inhibition [23, 24], only one of the two M-cells elicits an escape response at any one time. In accordance with this circuit design, previous studies have shown that after unilateral M-cell ablation, the probability of contralateral short-latency escape is decreased, with a concomitant increase in ipsilateral short-latency escapes [9]. Since spiral fiber neurons project to one M-cell only, we asked whether they also affect the escape behavior in a lateralized manner. To test this, we compared the effect of unilateral M-cell (Figure 3B) and spiral fiber neuron (Figure 3C) ablations on the directionality of the escape behavior in response to non-directional tap stimuli (Figure 3A). We expected that following the anatomy of the circuit, ablation of one M-cell or its contralateral spiral fiber neurons would bias escapes towards the ipsilateral and contralateral side with respect to the ablated somata, respectively (Figure 3E). We found that the overall frequency of short-latency escapes did not change following M-cell ablations (Figure 3D). However, as expected, unilateral M-cell ablations biased escapes towards one side (Figure 3F). Regardless of the original directional preference of individual fish before ablations, in all cases short-latency escapes contralateral to the ablated M-cell were virtually eliminated ($n = 11$, $35 \pm 9.0\%$ pre to $7.0 \pm 3.6\%$ post, Figure 3G). The directionality of the other, infrequent types of responses, such as long-latency escapes and swims, was not affected by the ablations (data not shown). Unilateral ablation of spiral fiber neurons had a similar effect as ablation of the M-cell they project to (Figure 3F). The percentage of short-latency escapes contralateral to the ablated spiral fiber neuron somata increased from $44 \pm 6.4\%$ to $91 \pm 4.1\%$ ($n = 17$, Figure 3G), while the overall fast-escape escape probability remained unchanged (Figure 3D). The laterality bias following M-cell or spiral fiber neuron ablation was not statistically distinguishable ($p > 0.05$). These experiments support the requirement of spiral fiber neurons for the normal functioning of their target M-cell.

Spiral fiber neuron activation enhances the probability of M-cell mediated escapes

Our results demonstrate that spiral fiber neurons are an essential excitatory input in the M-cell circuit. We next asked whether activating the spiral fiber neurons could decrease the threshold for M-cell mediated escapes. To test this hypothesis, we used *Tg(UAS:ChR2(H134R)-EYFP)* to express channelrhodopsin2 (ChR2) in neurons labeled in *Tg(-6.7FRhcrtR:gal4VP16)*. We measured larval responsiveness to low-intensity taps alone or paired with blue light. ChR2 excitation light was delivered via a blue laser beam focused on the fish's head 20–60 ms before the tap occurred and for a total of 100 ms (Figure 4A). We observed a strong enhancement of short-latency, M-cell mediated escapes in ChR2 positive fish when the weak taps were paired with blue light (4.4 fold enhancement, $p < 0.05$, Wilcoxon signed rank test), but not in controls lacking ChR2 (Figure 4B). In addition to modulating the probability of short-latency escapes, we reasoned that the excitatory effect of spiral fiber neurons on the M-cell might decrease escape latency. Indeed, short-latency escapes in response to taps paired with light occurred on average 0.95 ms earlier than those in response to taps alone in ChR2 positive fish ($p < 0.05$). Latency was not affected in ChR2 negative controls (Figure 4C). The probability of long-latency escapes was also moderately enhanced by pairing taps with blue light in ChR2 positive fish only (2.1 fold mean increase), likely due to unspecific ChR2-mediated effects. The latency of these escapes was not affected (Figures S3A and S3B).

To determine whether the ChR2-mediated enhancement of short-latency escapes was dependent on spiral fiber neurons, we tested behavior after spiral fiber neuron ablations. Short-latency escapes in response to taps alone were nearly abolished after spiral fiber neuron ablations, confirming our earlier ablation results. Crucially, pairing taps with blue light did not increase the probability of these escapes (Figure 4D). Our results suggest that spiral fiber neurons are necessary for the ChR2-mediated enhancement of M-cell mediated escapes.

We next asked whether excitation of spiral fiber neurons alone could evoke escape behaviors. In half of the larvae (11/22), a 100 ms blue light pulse gave rise to escapes with a probability above 10% (Figure 4E). Spiral fiber neuron ablations eliminated these escapes in all but one larva where lesions may have been incomplete. Optically induced escapes were kinematically similar to those induced by taps, but the angle of the initial C-bend was lower (Figures S3D and S3E), in agreement with reports that electrical stimulation of the M-cell alone gives rise to less effective escapes [25]. The latency from onset of blue light to behavior was long and variable (70 ± 30 ms, mean ± standard deviation, Figure 4F), which is not unusual for ChR2-mediated behavior [26–28] (but see [29]). The effectiveness of blue light correlated with escape latencies across fish (Figures S3F, S3G and S3H) and likely reflects ChR2 expression levels. Together, our optogenetic results indicate that exciting the spiral fiber neurons potentiates M-cell mediated behavior.

DISCUSSION

Our study unveils a functional pathway by which sensory information is indirectly conveyed to the escape circuit: spiral fiber neurons respond to aversive cues and excite the M-cell at the axon cap. We provide three lines of evidence that support the notion that spiral fiber

neurons are essential for M-cell mediated escapes: (1) like M-cell ablations, bilateral spiral fiber neuron ablations nearly abolish short-latency escapes; (2) ablating spiral fiber neurons unilaterally shifts the directionality of escapes; (3) optically activating spiral fiber neurons enhances M-cell mediated escapes in response to subthreshold stimuli. In the following sections, we relate our data to previous electrophysiological studies of the M-cell, discuss the utility of a spatially and temporally distinct convergent pathway, and describe how convergent pathways may be an important motif in neural circuits.

Spiral fiber neuron input is integrated with dendritic afferents at the M-cell axon hillock

Previous electrophysiological recordings in the goldfish have identified an input of unknown origin onto the M-cell [30]. Our findings suggest that this input has the characteristics of spiral fiber neuron excitation. In response to natural sounds, M-cell activity is composed of spatially and temporally distinct components: fast repetitive EPSPs are superimposed on an underlying slower depolarization [30]. Auditory/vestibular afferents making mixed electrical and chemical synapses on the M-cell lateral dendrites [31–33] are responsible for the fast component of the M-cell response and for part of the slower component [30]. The slower component also relies on an electrical and glutamatergic input near the soma [30], but the origin of this input is unknown. Spiral fiber neurons make both electrical and glutamatergic synapses close to the M-cell soma [10] and we find that they are active in response to sensory stimuli. This suggest that they are the origin of the secondary, slower component of the M-cell response, which was observed approximately 3 ms after the onset of the fast component. A 3 ms delay places this slower input within the M-cell's integration window: in response to auditory stimuli, initial depolarization in the goldfish M-cell occurs within 1 ms, but firing occurs from 3–12 ms [6, 34, 35]. Thus, in response to auditory/vibrational stimuli, excitatory inputs to the M-cell converge from two temporally and spatially distinct sources: distal sensory afferents provide rapid electrical and slower chemical input, and spiral fiber neurons provide a slow proximal input. Viral tracing experiments [36, 37] or other approaches are needed to identify the inputs of spiral fiber neurons.

To infer the site of integration of the dendritic and indirect inputs onto the M-cell, we recorded stimulus-elicited calcium activity in the M-cell soma before and after spiral fiber neuron ablations (Figure S4). We found that spiral fiber neuron ablations did not significantly affect calcium dynamics in the M-cell soma in response to taps, suggesting that dendritic inputs are responsible for the bulk of the somatic depolarization. Since spiral fiber neurons play a necessary role in M-cell mediated motor output, these experiments argue that inputs from spiral fiber neurons and direct sensory afferents are integrated at the level of the M-cell axon hillock to elicit an escape response (see supplementary results and discussion associated with Figure S4). Electrophysiological recordings of the M-cell axon and soma, and specific activation of spiral fiber neurons are needed to explicitly determine the nature of this spatiotemporal integration.

Spiral fiber neurons represent a convergent input that enhances circuit robustness

Short-latency escapes, which are triggered by a single firing event in the M-cell, are vital to avoid predation but should be restricted to legitimate threats. Therefore, the M-cell must be reliably activated when necessary and otherwise appropriately gated. The robust activation

of the M-cell is faced with three hurdles: first, due to a low input resistance, short time constant and hyperpolarized membrane potential, the M-cell requires strong currents to reach firing threshold [38]; second, feed-forward interneurons inhibit the M-cell [39, 40]; and third, dendritic excitation is strongly attenuated by the time it reaches the soma due to passive cable properties (up to 4-fold in the adult goldfish M-cell [30]). By providing an excitatory drive directly at the axon hillock, the site of action potential generation [41], spiral fiber neurons solve the challenge of overcoming the M-cell's high activation barrier. An additional challenge in the circuit is to ensure that the M-cell is not activated by innocuous short-lived sounds. Spiral fiber neurons introduce a delay line that may prevent unnecessary firing of the M-cell: transient depolarization of the M-cell by dendritic afferents would end before the necessary spiral fiber neuron input arrives at the axon hillock, precluding integration of the two pathways and rendering brief sensory input ineffective. Thus, in the M-cell escape circuit, indirect proximal input provides a necessary excitatory drive undiminished by distance and can serve as a mechanism to filter noise. Experiments combining stimulation of the two pathways and recordings in the M-cell are needed to directly test these scenarios.

Indirect excitatory pathways as a circuit motif

The spiral fiber neuron input is the first example of a necessary indirect pathway in a startle circuit. A diverse set of other circuits present anatomical similarities, where multiple, sometimes temporally and spatially segregated excitatory pathways converge. The interaction of inputs in these networks is poised to enhance the controllability and flexibility of the system, and may provide additional opportunities for modulation. A first example is the crayfish escape network, in which tactile afferents project to command neurons and also to excitatory interneurons that then feed forward to the command neurons. The amplitude of excitation elicited by the interneurons is larger than the excitation coming from direct tactile afferents [42], suggesting that like spiral fiber neurons in the M-cell circuit, these crayfish interneurons might be essential for producing escapes. Another example is the mammalian hippocampus where CA1 pyramidal neurons receive sensory information via a direct and an indirect pathway. One path projects monosynaptically onto the neurons' distal dendrites, but has a weak influence over somatic voltage. A slower trisynaptic pathway projecting to the proximal dendrites provides a stronger input [43]. Thus, similarly to spiral fiber neuron inputs in the M-cell circuit, the indirect pathway to CA1 introduces a powerful delay line that is more proximal. These examples of comparable circuitry in invertebrates and mammals suggest that the necessity of convergent excitatory pathways might be a general motif of neural circuits.

Supplementary Material

Refer to Web version on PubMed Central for supplementary material.

Acknowledgments

We thank Adam Douglass and Jared Wortzman for generating the *Tg(UAS:GCaMP5)* fish, Koichi Kawakami for the *Tg(UAS:GCaMP-HS)* line, Herwig Baier for the *Et(fos:Gal4-VP16)s1181t* line, Joel Greenwood and Edward Soucy for technical support with the behavioral apparatus, Steve Zimmerman, Karen Hurley, and Jessica Miller for fish care, Misha Ahrens, Elizabeth Carroll, Timothy Dunn, Joseph Fetcho, Minoru Koyama, Florian Merkle, Iris

Odstril, Yuchin Pan, Carlos Pantoja, Constance Richter, Kristen Severi, and additional members of the Engert and Schier labs for many helpful discussions. AML was supported by a Theodore H. Ashford Graduate Fellowships in the Sciences, an NSF Graduate Research Fellowship, and NIH T32HL007901. DS was supported by a Helen Hay Whitney Postdoctoral Fellowship and NIDCD K99DC012775. MH was supported by an EMBO Long Term Postdoctoral fellowship (ALTF 236 1056-10) and a postdoctoral fellowship by the Jane Coffin Childs Fund for Biomedical Research. OR was supported by an HFSP Long Term fellowship (LT000772/2012). CRW was supported by the Agency for Science, Technology and Research, Singapore. Research was supported by NIH grant R01HL109525 awarded to AFS.

References

1. Casagrand JL, Guzik AL, Eaton RC. Mauthner and reticulospinal responses to the onset of acoustic pressure and acceleration stimuli. J Neurophysiol. 1999; 82:1422–1437. [PubMed: 10482759]
2. Eaton RC, Lee RK, Foreman MB. The Mauthner cell and other identified neurons of the brainstem escape network of fish. Prog Neurobiol. 2001; 63:467–485. [PubMed: 11163687]
3. Pfaff DW, Martin EM, Faber D. Origins of arousal: roles for medullary reticular neurons. Trends Neurosci. 2012:1–9. [PubMed: 22217450]
4. Zottoli SJ, Faber DS. The Mauthner Cell: What Has it Taught us? The Neuroscientist. 2000; 6:26–38.
5. Korn H, Faber DS. The Mauthner cell half a century later: a neurobiological model for decision-making? Neuron. 2005; 47:13–28. [PubMed: 15996545]
6. Zottoli SJ. Correlation of the startle reflex and Mauthner cell auditory responses in unrestrained goldfish. J Exp Biol. 1977; 66:243–254. [PubMed: 858992]
7. Liu KS, Fetcho JR. Laser ablations reveal functional relationships of segmental hindbrain neurons in zebrafish. Neuron. 1999; 23:325–335. [PubMed: 10399938]
8. Kohashi T, Oda Y. Initiation of Mauthner- or non-Mauthner-mediated fast escape evoked by different modes of sensory input. J Neurosci. 2008; 28:10641–10653. [PubMed: 18923040]
9. Burgess HA, Granato M. Sensorimotor Gating in Larval Zebrafish. J Neurosci. 2007; 27:4984–4994. [PubMed: 17475807]
10. Koyama M, Kinkhabwala A, Satou C, Higashijima SI, Fetcho J. Mapping a sensory-motor network onto a structural and functional ground plan in the hindbrain. Proc Natl Acad Sci USA. 2011; 108:1170–1175. [PubMed: 21199937]
11. Kimmel CB, Sessions SK, Kimmel RJ. Morphogenesis and synaptogenesis of the zebrafish Mauthner neuron. J Comp Neurol. 1981; 198:101–120. [PubMed: 7229136]
12. Scott JW, Zottoli SJ, Beatty NP, Korn H. Origin and function of spiral fibers projecting to the goldfish Mauthner cell. J Comp Neurol. 1994; 339:76–90. [PubMed: 8106663]
13. Lorent K, Liu KS, Fetcho JR, Granato M. The zebrafish space cadet gene controls axonal pathfinding of neurons that modulate fast turning movements. Development. 2001; 128:2131–2142. [PubMed: 11493534]
14. Gyda M, Wolman M, Lorent K, Granato M. The Tumor Suppressor Gene Retinoblastoma-1 Is Required for Retinotectal Development and Visual Function in Zebrafish. PLoS Genet. 2012; 8:e1003106. [PubMed: 23209449]
15. Muto A, Ohkura M, Kotani T, Higashijima SI, Nakai J, Kawakami K. Genetic visualization with an improved GCaMP calcium indicator reveals spatiotemporal activation of the spinal motor neurons in zebrafish. Proc Natl Acad Sci USA. 2011; 108:5425–5430. [PubMed: 21383146]
16. O'Malley DM, Kao YH, Fetcho JR. Imaging the functional organization of zebrafish hindbrain segments during escape behaviors. Neuron. 1996; 17:1145–1155. [PubMed: 8982162]
17. Ikeda H, Delargy AH, Yokogawa T, Urban JM, Burgess HA, Ono F. Intrinsic properties of larval zebrafish neurons in ethanol. PLoS ONE. 2013; 8:e63318. [PubMed: 23658822]
18. Ernest S, Rauch GJ, Haffter P, Geisler R, Petit C, Nicolson T. Mariner is defective in myosin VIIA: a zebrafish model for human hereditary deafness. Hum Mol Genet. 2000; 9:2189–2196. [PubMed: 10958658]
19. Harris JA, Cheng AG, Cunningham LL, MacDonald G, Raible DW, Rubel EW. Neomycin-Induced Hair Cell Death and Rapid Regeneration in the Lateral Line of Zebrafish (Danio rerio). JARO - Journal of the Association for Research in Otolaryngology. 2003; 4:219–234.

20. Bianco IH, Ma LH, Schoppik D, Robson DN, Orger MB, Beck JC, Li JM, Schier AF, Engert F, Baker R. The tangential nucleus controls a gravito-inertial vestibulo-ocular reflex. Curr Biol. 2012; 22:1285–1295. [PubMed: 22704987]
21. Kohashi T, Nakata N, Oda Y. Effective Sensory Modality Activating an Escape Triggering Neuron Switches during Early Development in Zebrafish. J Neurosci. 2012; 32:5810–5820. [PubMed: 22539843]
22. Issa FA, O'Brien G, Kettunen P, Sagasti A, Glanzman DL, Papazian DM. Neural circuit activity in freely behaving zebrafish (Danio rerio). J Exp Biol. 2011; 214:1028–1038. [PubMed: 21346131]
23. Satou C, Kimura Y, Kohashi T, Horikawa K, Takeda H, Oda Y, Higashijima SI. Functional role of a specialized class of spinal commissural inhibitory neurons during fast escapes in zebrafish. J Neurosci. 2009; 29:6780–6793. [PubMed: 19474306]
24. Takahashi M, Narushima M, Oda Y. In vivo imaging of functional inhibitory networks on the mauthner cell of larval zebrafish. J Neurosci. 2002; 22:3929–3938. [PubMed: 12019312]
25. Nissanov J, Eaton RC, DiDomenico R. The motor output of the Mauthner cell, a reticulospinal command neuron. Brain Res. 1990; 517:88–98. [PubMed: 2376010]
26. Douglass AD, Kraves S, Deisseroth K, Schier AF, Engert F. Escape Behavior Elicited by Single, Channelrhodopsin-2-Evoked Spikes in Zebrafish Somatosensory Neurons. Current Biology. 2008; 18:1133–1137. [PubMed: 18682213]
27. Kubo F, Hablitzel B, Dal Maschio M, Driever W, Baier H, Arrenberg AB. Functional Architecture of an Optic Flow-Responsive Area that Drives Horizontal Eye Movements in Zebrafish. Neuron. 2014; 81:1344–1359. [PubMed: 24656253]
28. Thiele TR, Donovan JC, Baier H. Descending Control of Swim Posture by a Midbrain Nucleus in Zebrafish. Neuron. 2014; 83:679–691. [PubMed: 25066082]
29. Monesson-Olson BD, Browning-Kamins J, Aziz-Bose R, Kreines F, Trapani JG. Optical stimulation of zebrafish hair cells expressing channelrhodopsin-2. PLoS ONE. 2014; 9:e96641. [PubMed: 24791934]
30. Szabo TM, Weiss SA, Faber DS, Preuss T. Representation of auditory signals in the M-cell: role of electrical synapses. J Neurophysiol. 2006; 95:2617–2629. [PubMed: 16436476]
31. Nakajima Y. Fine structure of the synaptic endings on the Mauthner cell of the goldfish. J Comp Neurol. 1974; 156:379–402. [PubMed: 4137668]
32. Tuttle R, Masuko S, Nakajima Y. Freeze-fracture study of the large myelinated club ending synapse on the goldfish Mauthner cell: special reference to the quantitative analysis of gap junctions. J Comp Neurol. 1986; 246:202–211. [PubMed: 3007585]
33. Lin JW, Faber DS. Synaptic transmission mediated by single club endings on the goldfish Mauthner cell. I. Characteristics of electrotonic and chemical postsynaptic potentials. J Neurosci. 1988; 8:1302–1312. [PubMed: 2833580]
34. Eaton R, Lavender W. Identification of Mauthner-initiated response patterns in goldfish: evidence from simultaneous cinematography and electrophysiology. J Comp Physiol. 1981; 144:521–531.
35. Weiss SA, Zottoli SJ, Do SC, Faber DS, Preuss T. Correlation of C-start behaviors with neural activity recorded from the hindbrain in free-swimming goldfish (Carassius auratus). J Exp Biol. 2006; 209:4788–4801. [PubMed: 17114411]
36. Zhu P. Optogenetic dissection of neuronal circuits in zebrafish using viral gene transfer and the Tet system. Front Neural Circuits. 2009; 3:1–12. [PubMed: 19225575]
37. Mundell NA, Beier KT, Pan YA, Lapan SW, Göz Aytürk D, Berezovskii VK, Wark AR, Drokhlyansky E, Bielecki J, Born RT, et al. Vesicular stomatitis virus enables gene transfer and transsynaptic tracing in a wide range of organisms. J Comp Neurol. 2015
38. Curti S, Pereda AE. Functional specializations of primary auditory afferents on the Mauthner cells: interactions between membrane and synaptic properties. J Physiol Paris. 2010; 104:203–214. [PubMed: 19941953]
39. Zottoli SJ, Faber DS. An identifiable class of statoacoustic interneurons with bilateral projections in the goldfish medulla. Neuroscience. 1980; 5:1287–1302. [PubMed: 7402469]
40. Faber DS, Fetcho JR, Korn H. Neuronal networks underlying the escape response in goldfish. General implications for motor control. Ann N Y Acad Sci. 1989; 563:11–33. [PubMed: 2672948]

41. Furshpan EJ, Furukawa T. Intracellular and extracellular responses of the several regions of the Mauthner cell of the goldfish. J Neurophysiol. 1962; 25:732–771. [PubMed: 13945885]
42. Zucker RS. Crayfish escape behavior and central synapses. I. Neural circuit exciting lateral giant fiber. J Neurophysiol. 1972; 35:599–620. [PubMed: 5054506]
43. Dudman JT, Tsay D, Siegelbaum SA. A novel role for synaptic inputs at distal dendrites: instructive signals for hippocampal long-term plasticity. Neuron. 2007; 56:866–879. [PubMed: 18054862]

HIGHLIGHTS

- Spiral fiber neurons excite Mauthner cells, which mediate fast escape behavior
- Calcium imaging reveals that spiral fiber neurons encode aversive sensory cues
- Ablation and optogenetic experiments indicate that they are essential for escapes
- This study uncovers the crucial role of a feedforward excitatory motif for behavior

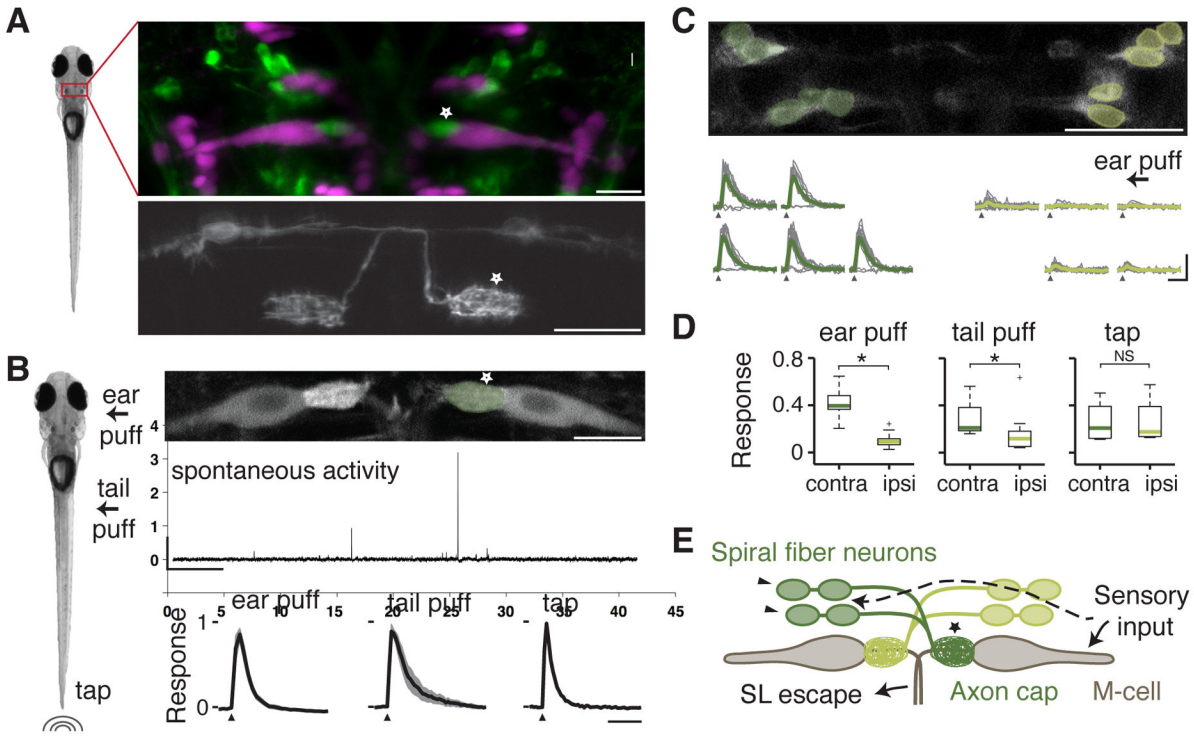

Figure 1. Spiral fiber neurons respond to aversive stimuli

A. Left image: 5 day old zebrafish larvae. Top image: *Tg(-6.7FRhcrtR:gal4VP16); Tg(UAS:GCaMP5)* labels spiral fiber neurons (arrowhead) among other neurons. The M-cell and other reticulospinal neurons are labeled with tetramethylrhodamine dextran by reticulospinal backfill. Spiral fiber neuron cell bodies are located in rhombomere 3 in two rostro-caudal (R↔C) clusters, approximately 25–40 μm rostral, 5–15 μm lateral, and 0–20 μm ventral of the axon cap. They all have axons descending contralaterally into the axon cap of the M-cell. Bottom image: Transient expression of membrane targeted GFP (*UAS:GAP43-GFP*) in *Tg(-6.7FRhcrtR:gal4VP16)* labels two spiral fiber neurons on the left and one spiral fiber neuron on the right that project to the contralateral M-cell axon cap (star).

B. Left image: 3 different stimuli were delivered to paralyzed zebrafish larvae: water puffs directed at the right ear, water puffs directed at the right side of the tail, and non-directional taps delivered onto the dish holding the fish. Top image: Projection of two-photon image stack showing M-cells and spiral fiber neuron axon terminals labeled with the calcium indicator *Tg(UAS:GCaMP-HS)* driven by *Et(fos:Gal4-VP16)s1181t* and *Tg(-6.7FRhcrtR:gal4VP16)* respectively. Middle panel: Typical spontaneous activity in the spiral fiber neuron axon terminals. Scale bars: 5 min horizontally, 1 Δf/f vertically. Bottom panel: Mean response amplitude in the right spiral fiber neuron axon terminals for different stimuli: ear puffs (n = 7, left panel), tail puffs (n = 5, middle panel), and taps (n = 6, right panel). For each fish, the change in fluorescence (Δf/f) from trials in which the axon cap was active was normalized to the maximum Δf/f across trials, and then averaged. The black line is the mean across fish with the standard error of the mean (SEM) shaded. Stimulus delivery is indicated by an arrowhead. Horizontal scale bar: 2 sec.

C. Top panel: Single recording plane showing spiral fiber neuron somata in *Tg(-6.7FRhcrtR:gal4VP16); Tg(UAS:GCaMP-HS)*. Bottom panel: Mean Δf/f across trials in green and individual trials in grey for spiral fiber neuron somata from the top panel located on the left (dark green) and on the right (light green) responding to a water puff delivered to the right ear (arrow). Contralateral spiral fiber neurons respond to the stimulus, but ipsilateral spiral fiber neurons do not. Traces in which spiral fiber neurons on the left do not respond correspond to the same trials. Note that while caudal neurons seem to respond before rostral neurons, this is an artifact of the delay introduced by 2-photon line scanning. Scale bars: 2 sec horizontally, 2 Δf/f vertically.

D. Boxplot showing the normalized response of spiral fiber neurons across fish. Response was defined as the area under the Δf/f curve over a 1.5 sec response window. This was normalized for each cell to the maximum response observed in a given experiment and then cells located on the contralateral (contra) and ipsilateral (ipsi) side with respect to the stimulus were averaged. Green lines are the medians across fish, box edges are the 25^{th} and 75^{th} percentiles, the whiskers extend to the most extreme data points not considered outliers, and crosses are outliers. Stimuli delivered: ear puffs (left panel, n = 10 fish, $p = 2.5*10^{-4}$), tail puffs (middle panel, n = 10, p = 0.02), and taps (right panel, n = 4, p = 0.89). * denotes $p < 0.05$, NS not significant by Wilcoxon rank sum test.

E. Model showing the M-cells receiving ipsilateral sensory input, which includes auditory/vestibular afferents onto the lateral dendrite. Our results suggest that spiral fiber neuron somata receive similar sensory information from the contralateral side.

Pictures are oriented rostral up; scale bars: 20 μm; arrows point to spiral fiber neuron somata; a star indicates spiral fiber neuron terminals at the M-cell axon cap. Abbreviations: contra: contralateral; ipsi: ipsilateral; SL: short-latency. See also Figure S1 and Movie S1.

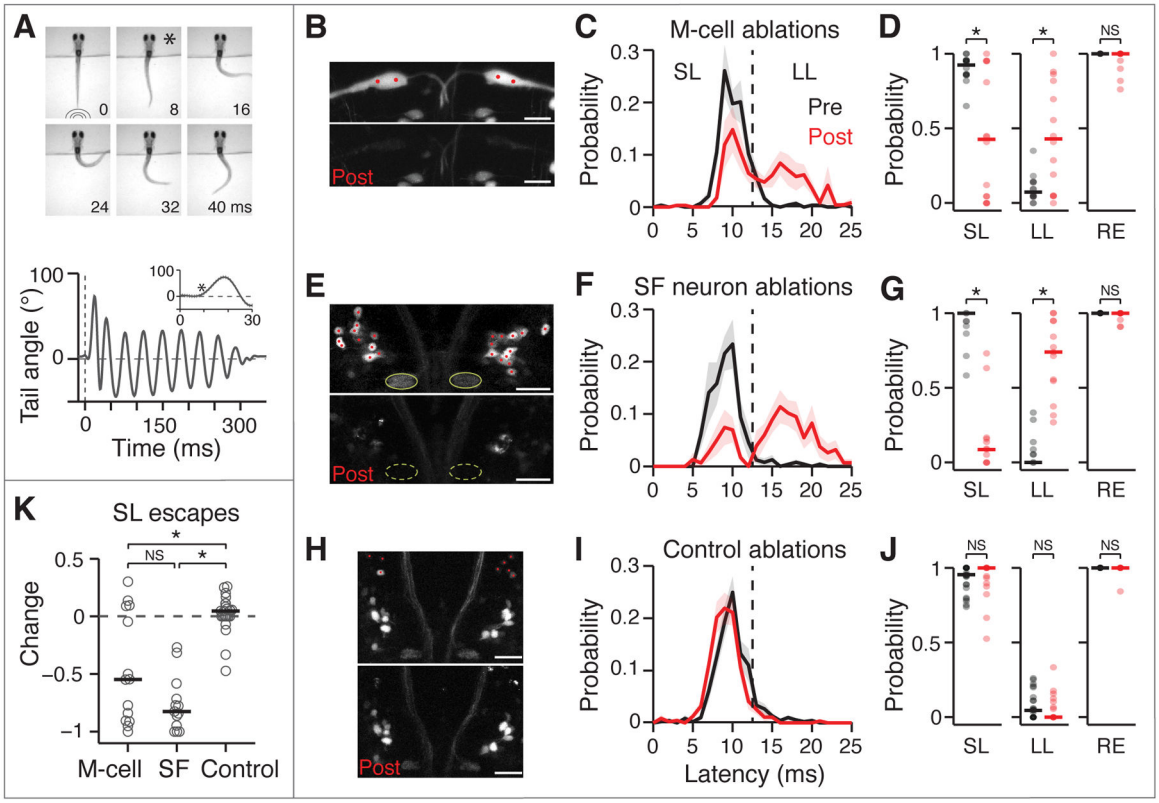

Figure 2. Loss of M-cells or spiral fiber neurons largely abolish short-latency escapes

A. Top image: Representative escape behavior of a head-embedded larval zebrafish responding to a tap stimulus. Images were recorded every millisecond and here every 8th image is shown. The first image was taken at the time the tap stimulus hit the dish holding the larvae. The image marked with a star corresponds to the beginning of the escape response (8 ms latency). Bottom panel: Representative smoothed tail trace showing the angle of the last tail segment with respect to the vertical in response to a tap. The escape behavior consists of a sharp angle C-bend, followed by a counter turn in the opposite direction and subsequent swimming lasting hundreds of milliseconds. The dotted line shows the stimulus. The inset shows the first 300 ms after stimulus onset and the star indicates the start of the C-bend.

B–J. Results of M-cell ablations (**B–D,** n = 14 fish), spiral fiber (SF) neuron ablations (**E–J,** n = 13) and control ablations (**H–J,** n = 23) on the escape behavior in response to taps. **B, E, H.** Stack projections showing before (top image) and immediately after (**B**) or 24 hours after (**E, H**) two-photon laser-mediated bilateral ablations (bottom image). **B.** *Et(fos:Gal4-VP16)s1181t; Tg(UAS:GCaMP-HS)*. **E**, **H.** *Tg(-6.7FRhcrtR:gal4VP16); Tg(UAS:Kaede)*. Red dots mark the cells or location within the M-cell that were targeted for ablation. Green ovals in **E** mark the axon caps, which are no longer apparent 24 hours after ablations. High fluorescence cell debris can be observed in the post images. **C, F, I.** Escape probability as a function of latency of all escapes performed, mean +/- SEM, before ablations (black) and after (red). The dotted line at 13 ms demarcates short- (SL, ≦ 12 ms) and long-latency (LL, 13–25 ms) escapes. **D, G, J.** Probabilities of different types of responses as a function of all

trials before (black) and after (red) ablations. Individual fish are displayed as semi-transparent dots and horizontal bars are the medians. Left: SL escapes; middle: LL escapes; right: overall responses (RE). M-cell: p = 0.013 pre vs. post (SL), 0.016 (LL) and 0.125 (RE); spiral fiber neuron: p = $2.4*10^{-4}$, $2.4*10^{-4}$, and 0.25; Control: p = 0.28, 0.20 and 1; Wilcoxon signed rank test.

K. Change in SL escape probability as a function of all trials (post-pre) based on the SL data plotted in **D, G, J.** Individual fish (grey circles), median (black line). M-cell vs. spiral fiber neurons: p = 0.11; M-cell vs. Control: p = 0.011; spiral fiber neurons vs. Control: p = $1.6*10^{-6}$, Wilcoxon rank sum test.

* denotes $p < 0.05$; NS not significant. Pictures are oriented rostral up; scale bars: 20 μm. Abbreviations: SF: spiral fiber; LS: short-latency; LL: long-latency; overall response. See also Figure S2.

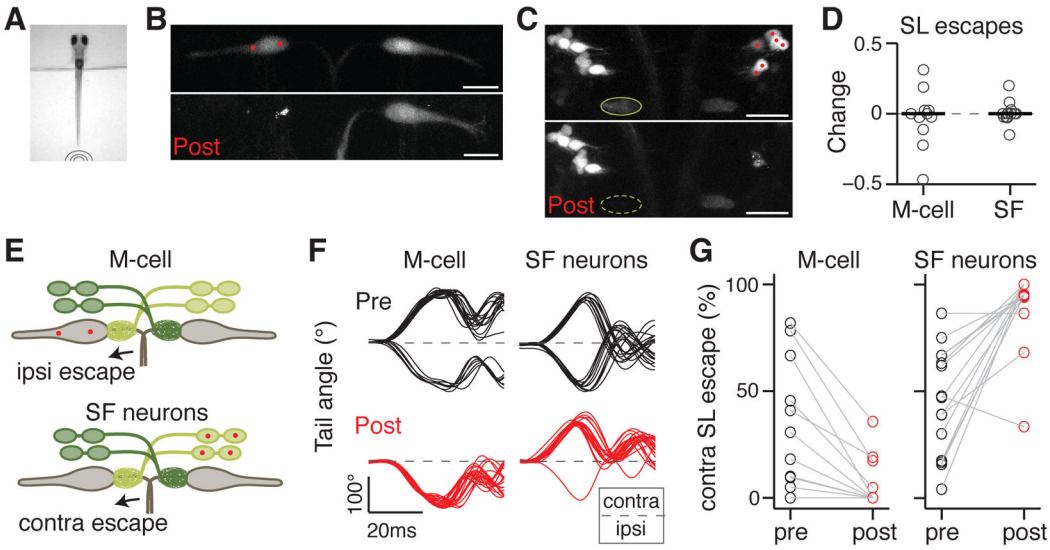

Figure 3. Spiral fiber neurons are necessary for lateralized M-cell mediated escapes

A. Tail free larvae are presented with a non-directional tap stimulus as in Figure 2.

B. Projection of two-photon image stack showing M-cells before (top image) and 24 hours after (bottom image) ablation of the M-cell on the left in *Et(fos:Gal4-VP16)s1181t; Tg(UAS:Kaede)*.

C. Projection of two-photon image stack showing spiral fiber neurons before (top image) and 24 hours after (bottom image) ablation of spiral fiber neuron somata located on the right in *Tg(-6.7FRhcrtR:gal4VP16); Tg(UAS:Kaede)*. The axon cap (green oval) contralateral to the targeted spiral fiber neurons is no longer apparent 24 hours after ablations.

D. Normalized change in short-latency (SL) escape probability as a function of all trials (post-pre/post+pre). Individual fish (grey circles) and median (black line). Left: M-cell ablation (n = 11). Right: spiral fiber neuron ablations (n = 17). The probability change is not significantly different from 0 in either condition (p = 0.67 and 0.98 respectively, Wilcoxon signed rank test).

E. Model showing that when M-cells or spiral fiber neurons are ablated unilaterally, escapes in response to taps become strongly biased towards one direction: ipsilateral to the ablated M-cell or contralateral to the ablated spiral fiber neurons.

F. Example tail traces for a fish before (top plots, black) and after (bottom plots, red) ablation of the left M-cell (left plots) and a fish before and after ablations of spiral fiber neuron somata on the right (right plots). The directionality of the initial tail bend is expressed as ipsilateral (ipsi) or contralateral (contra) with respect to the ablated soma(ta). Traces begin at the time of tap delivery.

G. Probability of contralateral SL escapes as a function of all SL escapes of either direction. Left panel: M-cell ablation. Right panel: spiral fiber neuron ablations. Escapes shift toward the ipsilateral side for M-cell ablation, and to the contralateral side for spiral fiber neuron ablations. The laterality bias following M-cell or spiral fiber neuron ablation was not statistically distinguishable (p = 0.45, Wilcoxon rank sum test).

Scale bars: 20 μm. Pictures are oriented rostral up. Abbreviations: SF: spiral fiber; LS: short-latency; contra: contralateral; ipsi: ipsilateral.

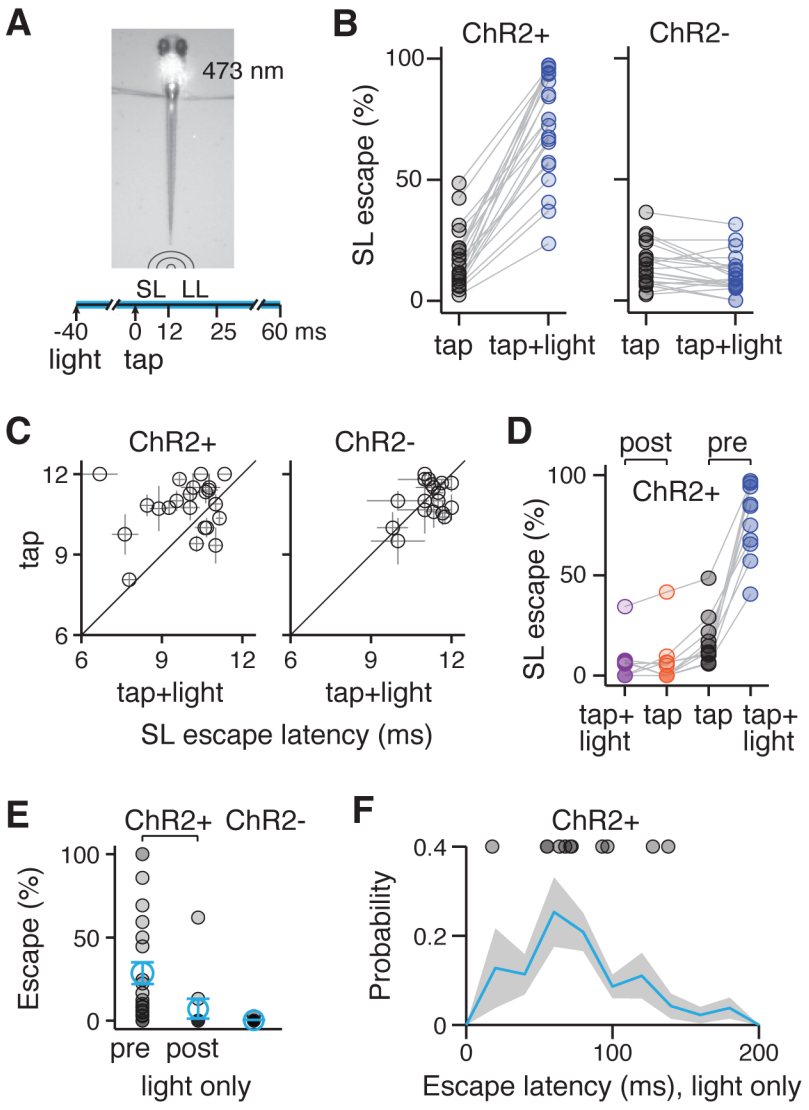

Figure 4. Activation of spiral fiber neurons enhances the probability of M-cell mediated escapes

A. 473 nm blue light is shone on the hindbrain of *Tg(-6.7FRhcrtR:gal4VP16); Tg(UAS:ChR2(H134R)-EYFP)* larvae using a focused laser beam for a total of 100 ms. 20–60 ms after the onset of the light, a low-intensity tap is delivered and tail movements are scored for short-latency (SL) or long-latency (LL) escapes.

B. % SL escapes for individual fish in response to taps alone (black circles) and taps paired with blue light (blue circles). Left panel: ChR2+ fish (n = 22, 17% ± 4.9% tap, 73.4% ± 4.7% tap + light, mean ± SEM, corresponding to a 4.4 fold enhancement of SL escapes with blue light, $p = 4.0*10^{-5}$). Right panel: ChR2- controls (n = 22, 15% ± 1.9% tap, 11% ± 1.7% tap + light, corresponding to a 1.4 fold decrease of SL escapes with blue light, p = 0.01, Wilcoxon signed rank test).

C. SL escape latency in ms in response to taps (y-axis) or taps paired with blue light (x-axis) for individual fish tested (black circles). Left panel: ChR2+ fish (n = 22, 11 ms ± 0.22 ms

tap, 9.9 ms ± 0.27 ms tap + light, mean ± SEM, p = 0.01). Right panel: ChR2- fish (n = 22, 11 ms ± 0.14 ms tap, 11 ms ± 0.13 ms ms tap + light, p = 0.72, Wilcoxon signed rank test).
D. % SL escapes in response to taps or taps paired with light before (pre) or after (post) bilateral spiral fiber neuron ablations. (n = 11 ChR+ larvae, pre: 17% ± 3.7% tap, 78 ± 5.4% tap + light, mean ± SEM, corresponding to a 4.7-fold enhancement, p = $9.8*10^{-4}$; post: 6.3% ± 3.5% tap, 5.6 ± 2.9% tap + light, p = 0.58, Wilcoxon signed rank test). Data in the pre condition are a subset of the data in B.
E. % Escapes for individual fish (black circles, mean ± SEM in blue) in response to blue light alone (in absence of taps). ChR2+ fish before (pre, n = 22) and after (post, n = 11) spiral fiber neuron ablations; ChR2- fish (n = 22).
F. Distribution of escape latencies in ChR2+ after the onset of a 100 ms blue light pulse (blue line ± shaded SEM, n = 185 escapes, 11 fish). Circles represent the mean of escape latencies for larvae displaying >10 % probability of escapes (see E pre, n = 11). Note: to ensure that escapes to blue light alone could be disambiguated with escapes in response to taps paired with light, larvae that responded to blue light alone with mean escapes latencies <70 ms were tested with a 20 ms delay between taps and blue light, otherwise, 40 or 60 ms delays were used (see **A**). See also Supplemental Experimental Procedures.
Abbreviations: ChR2: channelrhodopsin 2; LS: short-latency; LL: long-latency. See also Figure S3.